

# Exotic lensing corrections to the microlensing optical depth

J-F. Glicenstein

*DAPNIA-SPP, CE-Saclay, 91191 Gif-sur-Yvette, France*

## ABSTRACT

Microensing surveys derive the microlensing optical depth towards various directions such as the Galactic Centre from the distribution of observed Einstein radius crossing time. I show that the formula which is being used is invalid for “exotic” lensing events. The corrected formula is derived. The “parallax” effect (earth motion) requires no correction. Corrections for the finite size of the source and wide binary lenses are small (typically less than 1 %), except for blended events. Corrections for intermediate type binaries such as MACHO-LMC-9 can be substantial.

*Subject headings:* cosmology:dark matter — gravitational lensing

## 1. Introduction

Microensing surveys (Paczynski 1996) such as EROS, MACHO or OGLE have been very successful at finding microlensing candidates. The MACHO collaboration (Alcock et al. 2000a) found 13-17 events in their 5.7 year data sample towards the Large Magellanic Cloud (LMC). The EROS collaboration found 4 events towards the same direction in their 3 year data (Lasserre et al. 2000; Lasserre 2000) and 1 event in the 2 year Small Magellanic Cloud sample (Palanque-Delabrouille et al 1998). Hundreds of microlensing events were found by either MACHO (Alcock et al. 2000c) or OGLE (Wozniak et al. 2001) towards the Galactic Centre. EROS (Derue et al. 2001; Afonso 2001) found also tens of microlensing events towards the Galactic Disk and the Galactic Centre.

The microlensing optical  $\tau$  depth is given by

$$\tau = \int_0^{D_S} dD_d \pi r_E^2 \rho_d(D_d) \quad (1)$$

where  $D_d$  and  $D_S$  are the deflector and the source distance,  $\rho_d(D_d)$  is the number density of deflectors of mass  $M_d$  and  $r_E$ , the Einstein radius is given by

$$r_E = \sqrt{\frac{4GM_d D_d (D_S - D_d)}{c^2 D_S}} \quad (2)$$

The microlensing optical depth can be calculated towards any direction with a galactic model. An interesting property of the optical depth is that it is independent of the deflector mass function. Since the deflector mass function is not known precisely (it is totally unknown in the case of halo microlensing), the comparison between predicted and measured optical depths is little sensitive to systematics. The experimental determination of the optical depth is described in section 3.

The optical depth for microlensing towards the LMC measured by the MACHO collaboration is  $\tau_{LMC}^{MACHO} = 1.2_{-0.3}^{+0.4} 10^{-7}$ , a factor of 4 too small to explain the Galactic rotation curve. On the other hand, interpreting the observed optical depth in terms of lensing by known stellar populations in the galactic disk or in the LMC seems difficult, since the expected contribution is much smaller ( $\tau_{stellar} = 0.24 - 0.36 10^{-7}$ ). The optical depth towards the Baade window measured by MACHO with red giants is  $\tau = 2.0 \pm 0.4 10^{-6}$  (Popowski et al. 2000). This seems somewhat ( $\sim 30\%$ ) too large compared to the predictions of models (Evans et al. 2002). Previous measurements by MACHO (Alcock et al. 2000c) and OGLE (Wozniak et al. 20001) were even larger by a factor of 1.5-2.

Systematic effects have been suspected as the reason for the excess optical depth towards the LMC and the Galactic Centre. The main suspect is the "blending"<sup>1</sup> of source stars, sometimes associated with binary lensing effects (see e.g. (Di Stefano 2000)). The purpose of this paper is to investigate the role of "exotic" microlensing events in the calculation of the optical depth.

About 10% of the detected microlensing events are "exotic" events. They cannot be explained by the simplest "point lens-point source" (PLPS) model of lensing. Examples of exotic lenses are binary lenses or sources ("xallarap" events), "parallax" events (distorsion due to the earth motion around the sun), and events in which the disk of the source is differentially magnified (due to the finite size of the source). Since only 10% of the events are exotic, one naively expects a correction to the optical depth of at most 10% from exotic lensing. However, as will be shown in paragraph 4.3, the effect of exotic lensing is much stronger for blended events. Because of this, exotic events have a potentially large effect on the blending correction of the optical depth.

In the next two sections, I derive the expressions for the rate (equation (14b)) and the contribution to the optical depth (equation (21)) of exotic microlensing events.

---

<sup>1</sup>The objects monitored by microlensing surveys are blends of many stars whose seeing disk are overlapping. Any of these stars can be lensed. Optical depth estimates include in general a blending correction.

## 2. The microlensing rate

The Einstein radius crossing time  $t_E$  is the only physical information that can be obtained from most microlensing events. Once corrected for the experimental efficiency  $\epsilon(t_E)$ , the  $t_E$  distribution (or histogram) is an estimator  $d\hat{\Gamma}/dt_E$  of the differential microlensing rate  $d\Gamma/dt_E$ .

$$\frac{d\hat{\Gamma}}{dt_E} = \frac{1}{\epsilon(t_E)} \left( \frac{1}{N_{src} T_{obs}} \frac{dN_{micr}}{dt_E} \right) \quad (3)$$

where  $N_{src}$ ,  $T_{obs}$  and  $N_{micr}$  are the number of sources, the total observing time and the number of observed microlenses. A “lensing event” occurs whenever the magnification  $A$  of a microlensing event exceeds a threshold  $A_{thr}$  (in general  $A_{thr} = 1.34$ ). For a given source, the locus of lens positions for which  $A > A_{thr}$  is called the “microlensing tube” (Griest 1991). It is easy to show that the number of lenses  $dN$  at distance  $D_d$  entering the microlensing tube and crossing an area  $dl dD_d$  per unit time is

$$d\Gamma = \frac{d^2 N}{dt} = \rho_d v_t dl dD_d \cos\theta f(v_t) v_t dv_t d\theta \quad (4)$$

where  $\vec{v}_t$  is the transverse velocity of the lens,  $f(v_t)$  is the distribution of  $v_t = ||\vec{v}_t||$ ,  $\theta$  is the angle of  $\vec{v}_t$  with respect to the normal to the tube section and  $dl$  is the elementary length of the slice of the tube.  $v_t$  is related to  $t_E$  and  $r_E$  by

$$t_E = \frac{r_E}{v_t} \quad (5)$$

$d\Gamma$  is the number of lenses crossing inward an area  $dl dD_d$  of the microlensing tube per second. Hence this is not the microlensing event rate, since a lens may enter the microlensing tube several times. However, the difference between these two rates will be ignored until section 3.

The transverse velocity  $\vec{v}_t$  is the sum of 2 components: the microlensing tube transverse drift velocity  $\vec{v}_d$  and the velocity dispersion  $\vec{v}_{dis}$ .

$$\vec{v}_t = \vec{v}_d + \vec{v}_{dis} \quad (6)$$

I assume hereafter that the velocity dispersion is distributed according to

$$\tilde{f}(\vec{v}_{dis}) = \frac{1}{2\pi\sigma_x\sigma_y} \exp\left(-\left(\frac{v_{dis(x)}^2}{2\sigma_x^2} + \frac{v_{dis(y)}^2}{2\sigma_y^2}\right)\right) \quad (7)$$

where  $x$  and  $y$  are the eigendirections of the velocity dispersion tensor.  $\tilde{f}$  is normalized by

$$\int \tilde{f} dv_{dis(x)} dv_{dis(y)} = 1 \quad (8)$$

The orientation of the microlensing tube is arbitrary relative to the eigendirections of the velocity tensor. The transverse velocity distribution has to be averaged over all the orientations of the microlensing tube.

If the velocity dispersion tensor is isotropic with  $\sigma_x = \sigma_y = \sigma$ , the  $v_t$  distribution is given by

$$f(v_t) = \frac{1}{2\pi\sigma^2} \exp\left(-\frac{1}{2\sigma^2}(v_t^2 + v_d^2 - 2v_tv_d \cos(\gamma + \Psi - \beta))\right) \quad (9)$$

where the angles  $\gamma$ ,  $\Psi$  and  $\beta$  are defined in figure 1. Averaging over  $\alpha = \beta - \delta$  at fixed  $\gamma$ ,  $\Psi$  and  $\delta$  gives:

$$\bar{f}(v_t) = \frac{1}{2\pi} \int_0^{2\pi} d\alpha f(v_t) = \frac{1}{2\pi\sigma^2} \exp\left(-\frac{1}{2\sigma^2}(v_t^2 + v_d^2)\right) I_0\left(\frac{2v_tv_d}{\sigma^2}\right) \quad (10)$$

where  $I_0$  is a modified Bessel function.

The general expression of  $\bar{f}$  is cumbersome and derived in the appendix. It depends only on the kinematical variable  $v_d$  and is independent of the geometry of the microlensing tube.

Changing variable from  $v_t$  to  $t_E$  and integrating over  $\theta$  gives:

$$d\Gamma = 2\rho_d dl dD_d \left(\frac{r_E^3}{t_E^4}\right) dt_E \bar{f}\left(\frac{r_E}{t_E}\right) \quad (11)$$

Since  $\bar{f}(v_t)$  is independent of the geometry of the lensing tube, the integration over  $l$  is trivial:

$$d\Gamma = 2\rho_d l dD_d \left(\frac{r_E^3}{t_E^4}\right) dt_E \bar{f}\left(\frac{r_E}{t_E}\right) \quad (12)$$

For a PLPS, the microlensing tube section is a circle with length  $l = 2u_{min}\pi r_E$  with  $u_{min}$  given by

$$u_{min} = \sqrt{2} \sqrt{(A_{thr} / \sqrt{A_{thr}^2 - 1}) - 1}$$

For a general lens, the tube section is much more complicated. On dimensional grounds, the length  $l$  of the lensing tube can be written as

$$l = 2\pi r_E K(A_{thr}) \quad (13)$$

The K factor is a function of both the magnification threshold  $A_{thr}$  and the geometry of the lens (e.g the distance of the components in Einstein units and the mass ratio of the components for a binary lens). K is not in general linear in  $u_{min}$ . For instance, for a binary lens and  $A_{thr} \gg 1$ , K is almost independent of  $u_{min}$  (see section 4.3).

Replacing  $l$  from equation (13) into equation (12) gives:

$$d\Gamma = 4\pi K(A_{thr})\rho_d dD_d \left(\frac{r_E^4}{t_E^4}\right) dt_E \bar{f}\left(\frac{r_E}{t_E}\right) \quad (14a)$$

$$= K(A_{thr})\left(\frac{d\Gamma}{dt}\right)_0 dt_E \quad (14b)$$

where  $(\frac{d\Gamma}{dt})_0$  is the rate obtained with point sources and point lenses. Equation (14b), which was also found by Baltz and Gondolo (Baltz and Gondolo 2001) means that the lensing rate for exotic lenses can be calculated by rescaling the lensing rate for PLPS lenses with  $K$ .  $K$  can be calculated for any observed microlensing event, provided the geometry of the event and the magnification threshold  $A_{thr}$  are known. Examples of calculations are given in section 4.1 and 4.2.

If source stars are not resolved and differential photometry is used, the magnification threshold depends on the magnitude of the source star and has to be found on an event-by-event basis. From now on, I assume that the microlensing events are found by monitoring a catalog of resolved objects and using a fixed magnification threshold. The resolved objects are a blend of many stars. If only a fraction  $f$  of the source object flux is magnified, it is useful to define an effective magnification threshold by

$$A_{thr}^{eff} = \frac{A_{thr} + f - 1}{f} \quad (15)$$

### 3. Estimation of the microlensing optical depth

For the purpose of calculating  $\tau$ , it is convenient to calculate a weighted average of  $t_E$ . One gets from equation (3):

$$\langle t_E \rangle = \int \left(\frac{1}{K} \frac{d\Gamma}{dt_E} t_E dt_E\right) \quad (16)$$

$$= \frac{1}{N_{src} T_{obs}} \sum_{events} \frac{p}{K(A_{thr})} \frac{t_E}{\epsilon(t_E)} \quad (17)$$

Since  $d\Gamma/dt_E$  is the number of lenses entering the microlensing tube per unit time and unit  $t_E$ , the observed events in the r.h.s of equation 17 have (in general) to be multiply counted. The multiplicity  $p$  is the number of observed amplification threshold crossings.

The experimental efficiency takes into account the loss of events due the selection cuts (see e.g. (Lasserre 2000)) as well as time sampling. It is generally calculated with simulated microlensing light curves superimposed to observed stable star light curves. It is thus clear that the experimental efficiency depends not only on  $t_E$ , but also on the geometry of the lensing event and needs not be the same for binaries and PLPS lenses.

Inserting equation (14b) in the r.h.s of equation (16) gives

$$\frac{1}{N_{src}T_{obs}} \sum_{events} \frac{p}{K(A_{thr})} \frac{t_E}{\epsilon(t_E)} = -4\pi \int \rho_d dD_d \int \left(\frac{r_E^4}{t_E^3}\right) dt_E \bar{f}\left(\frac{r_E}{t_E}\right) \quad (18)$$

Changing variable from  $t_E$  to  $w = r_E/t_E$  one gets:

$$\frac{1}{N_{src}T_{obs}} \sum_{events} \frac{p}{K(A_{thr})} \frac{t_E}{\epsilon(t_E)} = 4 \int \pi \rho_d r_E^2 dD_d \int dw w \bar{f}(w) \quad (19)$$

$$= 4(\int dw w \bar{f}(w))\tau \quad (20)$$

The integral over  $w$  is calculated in the appendix. The r.h.s of equation (20) is independent of  $v_d$ ,  $\sigma_x$  and  $\sigma_y$ . Equation (20) can be rewritten as

$$\tau = \frac{\pi}{2N_{src}T_{obs}} \sum_{events} \left(\frac{p}{K(A_{thr})}\right) \frac{t_E}{\epsilon(t_E)} \quad (21)$$

Equation (21) is the main result of this paper and will be fully discussed in the next section. For PLPS lenses,  $K$  is simply  $u_{min}$ . For  $K = u_{min} = p = 1$ , equation (21) gives the formula used by the microlensing surveys to derive  $\tau$  from the observed Einstein radius crossing time distribution. As far as the authors know, exotic microlensing events have always been either summed up as ordinary events or just ignored. I now estimate the values of  $K$  for exotic lenses.

## 4. Discussion

As explained in the introduction, many types of exotic microlensing events have been observed. The earth motion on its orbit around the sun ("parallax") is detected as a small asymmetry on the light curve of microlensing events. The weight for parallax events is simply  $K = 1$ , because the  $K$  factor is independent of the lensing tube drift velocity  $v_d$ . By the same argument, "xallarap" events which are the motion of the source around a companion also have  $K = 1$ .

The main effects which require a non trivial value of  $K$  are the finite size of source stars and binary lenses. To give specific values, I now take as example the events found by the MACHO collaboration (Alcock et al. 1997; Alcock et al. 2000a) towards the LMC. Three events in the MACHO sample are possible exotic events (Dominik and Hirschfeld 1996; Alcock et al. 2000b): LMC-1 (finite size or binary lensing), LMC-9 (binary lensing) and

LMC-10 (binary lensing). Note that LMC-9 and LMC-10 were used for estimating the microlensing optical depth towards the LMC in the 2 year sample (Alcock et al. 1997), but were discarded in the 5.7 year sample (Alcock et al. 2000a). The magnification threshold was  $A_{thr} = 1.75$  in the 2 year sample and  $A_{thr} = 1.49$  in the 5.7 year sample. Event LMC-1 can be taken as unblended. Event LMC-9 has blending coefficients in the R and B band of  $f_R \simeq 0.26$  and  $f_B \simeq 0.17$  (Alcock et al. 2000b) so that its effective magnification threshold is  $A_{thr}^{eff} \simeq 3.4$ . Event LMC-10 has blending coefficients of  $f_B = f_R = 0.15$  and the effective magnification threshold is  $A_{thr}^{eff} \simeq 4.3$ .

#### 4.1. Finite size of source stars

The magnification of extended sources depends in a complicated way on  $\sigma = r_s D_S / r_E D_d$  (Witt and Mao 1994), where  $r_s$  is the source star radius. MACHO event LMC-1 shows a deviation to the simplest PLPS microlensing model. This deviation has been modeled by various authors (Witt and Mao 1994; Dominik and Hirschfeld 1996) as the effect of the source disk finite extent. A value of  $\sigma \simeq 0.18$  has been fitted by Dominik and Hirschfeld (Dominik and Hirschfeld 1996).

The microlensing light curve with extended sources has been calculated by Witt and Mao (Witt and Mao 1994). In the limit  $\sigma \ll 1$ , they find that the extended source light curve is a simple extension of the PLPS light curve (equation (A4) of (Witt and Mao 1994))

$$A_{thr}^{MACHO} = \frac{2 + K^2}{K \sqrt{4 + K^2}} + \sigma^2 \frac{4(1 + K^2)}{K^3(4 + K^2)^{(5/2)}} \quad (22)$$

Solving equation (22) for K and comparing with the usual impact parameter  $u_{min}$  which is the solution of

$$A_{thr}^{MACHO} = \frac{2 + u_{min}^2}{u_{min} \sqrt{4 + u_{min}^2}} \quad (23)$$

gives  $K_{LMC-1}^{fs} = 1.008 u_{min}$ .

The value K correction is thus within 1% of  $u_{min}$  in spite of the relatively large  $\sigma$  value assumed here. However, as shown in section 4.3, the K correction for a finite source effect may become important for a strongly blended source star.

#### 4.2. Binary lenses

In cases more complicated than the finite size effect, such as binary lenses (Schneider and Weiss 1986; Mao and Paczyński ; Dominik 1999), the microlensing tube has

a complicated shape. The total length  $l$  of the tube section has been calculated by a Monte-Carlo algorithm. A small “rod” with length  $\lambda$  is generated in the source plane and rotated around its center. The magnification is calculated at both ends of the “rod”. The fifth order equation giving the magnification of binary lenses (Witt and Mao 1995) is solved numerically. The points selected are those for which one end of the rod is above threshold and the other is under. These points cover an area  $\mathcal{A}$  of width  $2\lambda$  having the shape of a ribbon located along the tube slice boundary, equally spread on each side of this boundary.

The length  $l$  is thus found by  $l = \mathcal{A}/(2\lambda)$ .

I find that the K correction for LMC-1 is consistent with 1 at the 1% level in both MACHO binary models 1a and 1b. The K corrections for LMC-9 and LMC-10 are:

$$K_{LMC-9}(1.75) = (1.49 \pm .04)u_{min} \quad (24a)$$

$$K_{LMC-10}(1.75) = (1.11 \pm .03)u_{min} \quad (24b)$$

for the 2 year analysis and

$$K_{LMC-9}(1.49) = (1.31 \pm .06)u_{min} \quad (25a)$$

$$K_{LMC-10}(1.49) = (1.06 \pm .01)u_{min} \quad (25b)$$

for the 5.7 year analysis.

First assume that the efficiencies and blending corrections calculated with PLPS lenses can be used on binary lenses. Then the optical depth contributed by events LMC-9 and LMC-10 can be obtained by dividing the values in table 7 of (Alcock et al. 1997) and table 8 of (Alcock et al. 2000a) by the relevant K factors. The microlensing optical depth of (Alcock et al. 1997) is changed from  $\tau = 2.9 \cdot 10^{-7}$  to  $\tau = 2.65 \cdot 10^{-7}$ , a 8% effect. The optical depth of analysis B of (Alcock et al. 2000a) is lowered by only 2%. In both cases, the effect is much smaller than the systematics quoted in the papers.

However, the reductions of the optical depth by 8% and 2% are only lower limits, because the blending corrections increase the detection efficiency of binaries such as LMC-9 and LMC-10 more than that of PLPS lenses. This can be seen by calculating the K factors at the effective magnification threshold  $A_{thr}^{eff}$  instead of the magnification threshold  $A_{thr}$ . The K factors are:

$$K_{LMC-9}(3.4) = (2.9 \pm .1)u_{min} \quad (26a)$$

$$K_{LMC-10}(4.3) = (1.9 \pm .1)u_{min} \quad (26b)$$

The increase in lensing rate of binary lenses relative to PLPS (measured by K) has to be taken into account in the blending correction of the detection efficiency.



An important question is whether lenses with distant companions (“wide binaries”) have any K corrections, since a large ( $\sim 50\%$ ) fraction of the stars are members of binary systems. The simulation shows that the K correction for a binary star with mass ratio  $q$  and projected separation  $a$  is within 1% of 1 (assuming  $A_{thr} = 1.34$ ) as long as

$$\frac{q r_E^2}{a^2} < 0.1 \quad (27)$$

Assuming that the projected separation is half the space separation and using Kepler’s third law, this condition can be recast as a constraint on the period  $P$  of the binary :

$$P > 452(qx(1-x))^{3/4} \left(\frac{M_d}{M_\odot}\right)^{1/4} \left(\frac{D_s}{10 \text{ kpc}}\right)^{3/4} \text{ yr} \quad (28)$$

where  $x = D_d/D_s$ . Taking  $q = 0.5$ ,  $M_d = 0.2 M_\odot$ , and typical values  $1 - x = 6 \cdot 10^{-2}$  ( $x = 0.85$ ) for LMC (Galactic Centre) lenses, the constraint on  $P$  becomes  $P > 50 \text{ yr}$ . The  $\log P$  distribution for binaries is roughly gaussian with an average period  $P_{av} \sim 6 \cdot 10^4$  days and  $\sigma_{\log P} = 2.3$  (Duquennoy and Mayor 1991). Thus roughly 62% of the binary lenses do not need a K correction for an unblended source and a magnification threshold  $A_{thr} = 1.34$ . As will be seen in the next section, the conclusion that a large fraction of wide binaries do not need to be corrected remains valid for blended sources.

### 4.3. Blending

The examples of LMC-9 and LMC-10 show that  $K/u_{min}$  can be much larger than 1 for blended sources. This can be easily understood for binary lenses, since the length of the microlensing tube tends to twice the caustics length at high  $A_{thr}$  (neglecting the finite size of the source) instead of 0 for PLPS lenses. For wide binaries in the high  $A_{thr}$  limit, the caustic length is  $\sim 8\sqrt{2}q(r_E/a)^2 r_E$  (Dominik 1999) so that the K factor is :

$$\frac{K}{u_{min}} \simeq \frac{8\sqrt{2}}{\pi u_{min}} q \left(\frac{r_E}{a}\right)^2 \simeq 3.6q A_{thr} \left(\frac{r_E}{a}\right)^2 \quad (29)$$

For a strongly blended source star with  $A_{thr}^{eff} \sim 1000$ , the condition  $K/u_{min} > 1$  gives a constraint on the period  $P > 10^4 \text{ yr}$ . In other words, even with  $A_{thr}^{eff} \sim 1000$ , one third (roughly) of binary lenses need not be K corrected. But the correction for the other binary lenses, especially intermediate type binaries such as MACHO LMC-9 may be very large.

The finite size of blended source stars can give non negligible values for  $K/u_{min} - 1$ . Numerically,  $K/u_{min}$  is found to depend only on  $\sigma A_{thr}$ , where  $\sigma$  is defined in section 4.1.

The variation of  $K/u_{min}$  as a function of  $\sigma A_{thr}$  is shown in figure 2. Figure 2 is very similar to figure 3 of (Schneider 1987) and the underlying physics is of course the same.

A LMC lens with  $M_d = 0.1M_\odot$  located at 300 pc in front of the source has an Einstein radius  $r_E \simeq 0.5\text{AU}$ . The parameter  $\sigma$  ranges from 0.1 for a red giant source to  $10^{-3}$  for a M dwarf. These relatively high  $\sigma$  values may give non-trivial K factors. For instance, a solar type star inside the seeing disk of a giant star contributes only  $\sim 1/100$  of the total light. The magnification threshold for such a star is thus  $\sim 100$  and the K factor is  $\sim 1.2u_{min}$  from figure 2.

A  $0.1M_\odot$  lens located 1500 pc in front of the Galactic Centre has an Einstein radius of  $r_E \simeq 1\text{AU}$ , so that the orders of magnitude are similar to those discussed in the previous paragraph.

In microlensing surveys, the raw efficiencies and Einstein radius crossing time are generally modified to take the “blending” of sources into account (Alcock et al. 2001). K factors generally increase the efficiency for detecting blended sources and thus tend to decrease the optical depth.

## 5. Conclusion

Exotic microlensing events such as binary lensing or source finite size effects contribute differently from the simplest “point lens-point source” events to the optical depth. Taking this effect into account leads to a reduction in the measured optical depth. The finite size of blended stars may give a reduction of up to 30% of the microlensing optical depth. The effect of binaries may be even larger. Thus correcting with K factors might reduce the disagreement between measurements and models towards the Galactic Center and the LMC.

I am grateful to Andy Gould, Jacques Haissinski and Jim Rich for many interesting comments. I also thank Clarisse Hamadache for helpful suggestions.

## A. Appendix

The direction of the principal axis of the velocity dispersion tensor relative to arbitrary axis (X,Y) is given by the angle  $\alpha$ . The direction of drift by the angle  $\beta = \alpha + \delta$ . One has:

$$v_{(dis)_x} = v_t \cos(\gamma + \Psi - \alpha) - v_d \cos \delta \tag{A1}$$

$$v_{(dis)_y} = v_t \sin(\gamma + \Psi - \alpha) - v_d \sin \delta \tag{A2}$$

(A3)

Rotating the microlensing tube is equivalent to rotating the (X,Y) axis system or  $\alpha$ . Hence, using equation 7, averaging over  $\alpha$  and keeping  $\gamma$ ,  $\Psi$  and  $\delta$  fixed gives

$$\bar{f}(v_t) = \frac{1}{(2\pi)^2 \sigma_x \sigma_y} \int_0^{2\pi} \exp[-1/2(\frac{(v_t \cos \alpha - v_d \cos \delta)^2}{\sigma_x^2} + \frac{(v_t \sin \alpha + v_d \sin \delta)^2}{\sigma_y^2})] d\alpha \quad (\text{A4})$$

$\bar{f}$  depends only on  $v_d$  and is independent of the geometry of the microlensing tube. In section 2, it has been shown that  $\tau$  is equal to  $\sum_{events} \frac{1}{K(A_{thr})} \frac{t_E}{\epsilon(t_E)}$  up to a numerical factor which is the integral

$$I(\bar{f}) = \int dw w \bar{f}(w) \quad (\text{A5})$$

Defining  $w'$ ,  $\alpha'$ ,  $\delta'$  and  $v'_d$  as

$$w' = \sqrt{\frac{\cos^2 \alpha}{\sigma_x^2} + \frac{\sin^2 \alpha}{\sigma_y^2}} w \quad (\text{A6})$$

$$\tan(\alpha') = \frac{\sigma_x}{\sigma_y} \tan(\alpha) \quad (\text{A7})$$

$$\tan(\delta') = \frac{\sigma_x}{\sigma_y} \tan(\delta) \quad (\text{A8})$$

$$v'_d = \sqrt{\frac{\cos^2 \delta}{\sigma_x^2} + \frac{\sin^2 \delta}{\sigma_y^2}} v_d \quad (\text{A9})$$

and changing variable from  $(w, \alpha)$  to  $(w', \alpha')$  gives

$$I(\bar{f}) = \frac{1}{(2\pi)^2} \int_0^\infty dw' w' \int_0^{2\pi} d\alpha' \exp[-1/2(w'^2 + (v'_d)^2 - 2w'v'_d \cos(\alpha' - \delta'))] \quad (\text{A10})$$

Next integrating over  $\alpha'$  gives:

$$I(\bar{f}) = \frac{1}{2\pi} \int_0^\infty dw' w' \exp[-1/2(w'^2 + (v'_d)^2)] I_0(w'v'_d) \quad (\text{A11})$$

Using equation 11.4.29 of Gradshteyn and Ryzhik ((Gradshteyn and Ryzhik 1980)) yields finally:

$$I(\bar{f}) = \frac{1}{2\pi} \quad (\text{A12})$$

## REFERENCES

Paczynski, B. 1996, Ann. Rev. Astron. Astrophys. 34

Lasserre, T. et al. 2000, A&A, 355, L39

- Lasserre, T. 2000, PhD. thesis, Université de Paris 6
- Alcock, C. et al. 2000, ApJ 542, 281
- Palanque-Delabrouille, N. et al 1998, A&A332,1
- Alcock, C. et al. 2000, ApJ 541, 734
- Wozniak, P.R. et al. 2001, Acta Astronomica, 51,175
- Popowski, P. et al. 2000, in “Microlensing 2000: a New Era in Microlensing Astrophysics”, ASP Conference Series, J.W Menzies & P.D.Sackett eds.
- Evans, N.W. & Belokurov, V 2002, ApJ567, L19
- Derue, F. et al 2001, A&A373, 126
- Afonso, C. 2001, PhD. thesis, Université de Paris 7
- Di Stefano, R. 2000, ApJ 541, 587
- Griest, K. 1991, ApJ 366, 412
- Baltz, E.A & Gondolo, P. 2001, ApJ 559, 41
- Alcock, C. et al. 1997, ApJ 486, 697
- Alcock, C. et al. 2000, ApJ 541, 270
- Dominik, M. & Hirschfeld, A.C., 1996, A&A, 313, 841
- Witt, H.J & Mao, S. 1994, ApJ 430, 505
- Schneider, P. & Weiss, A. 1986, A&A 164, 237
- Mao, S. & Paczyński, B. 1991, ApJ 374, L37
- Dominik, M. 1999, A&A 349, 108
- Witt, H.J & Mao, S. 1995, ApJ 447, 105
- Duquennoy, A. & Mayor, M., A&A248, 485 (1991)
- Schneider, P. 1987, A&A 179,71
- Alcock, C. et al. 2001, ApJS 136, 439

Gradshteyn I.S.G, & Ryzhik, I.M 1980, Table of Integrals, Series and Products, Academic Press, New York

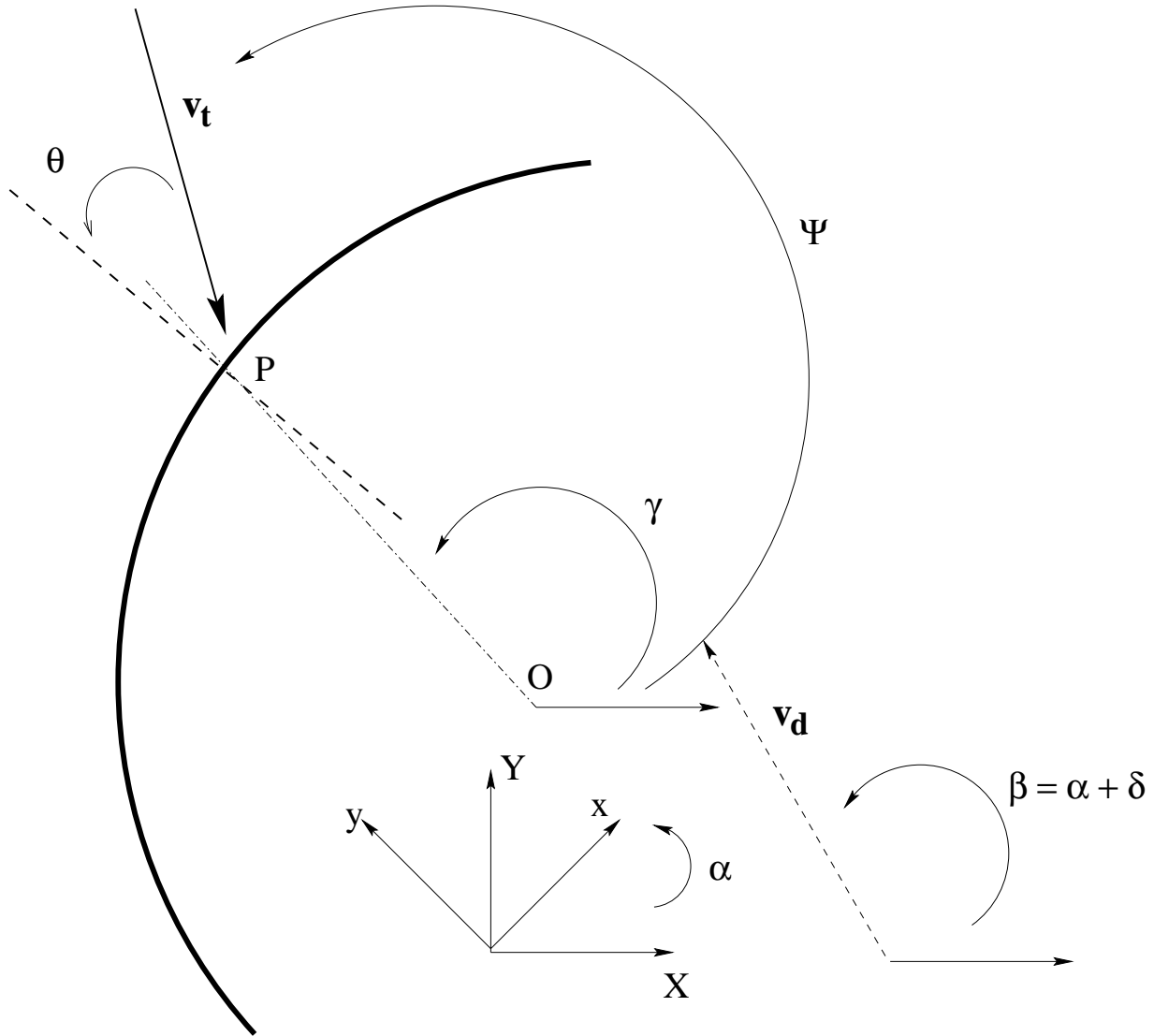


Fig. 1.— Section of the microlensing tube (thick line) perpendicular to the line of sight. The point  $O$  and the  $X, Y$  axes are arbitrary. The point  $P$  is on the microlensing tube. The velocity tensor at  $P$  has principal axes  $x, y$ . The normal to the slice of the microlensing tube is shown by the dashed line and is oriented outwards. The angle between  $X$  and  $x$  is  $\alpha$ . The drift velocity of the tube projected in a plane perpendicular to the line of sight  $\vec{v}_d$  makes an angle  $\beta$  with  $X$ .

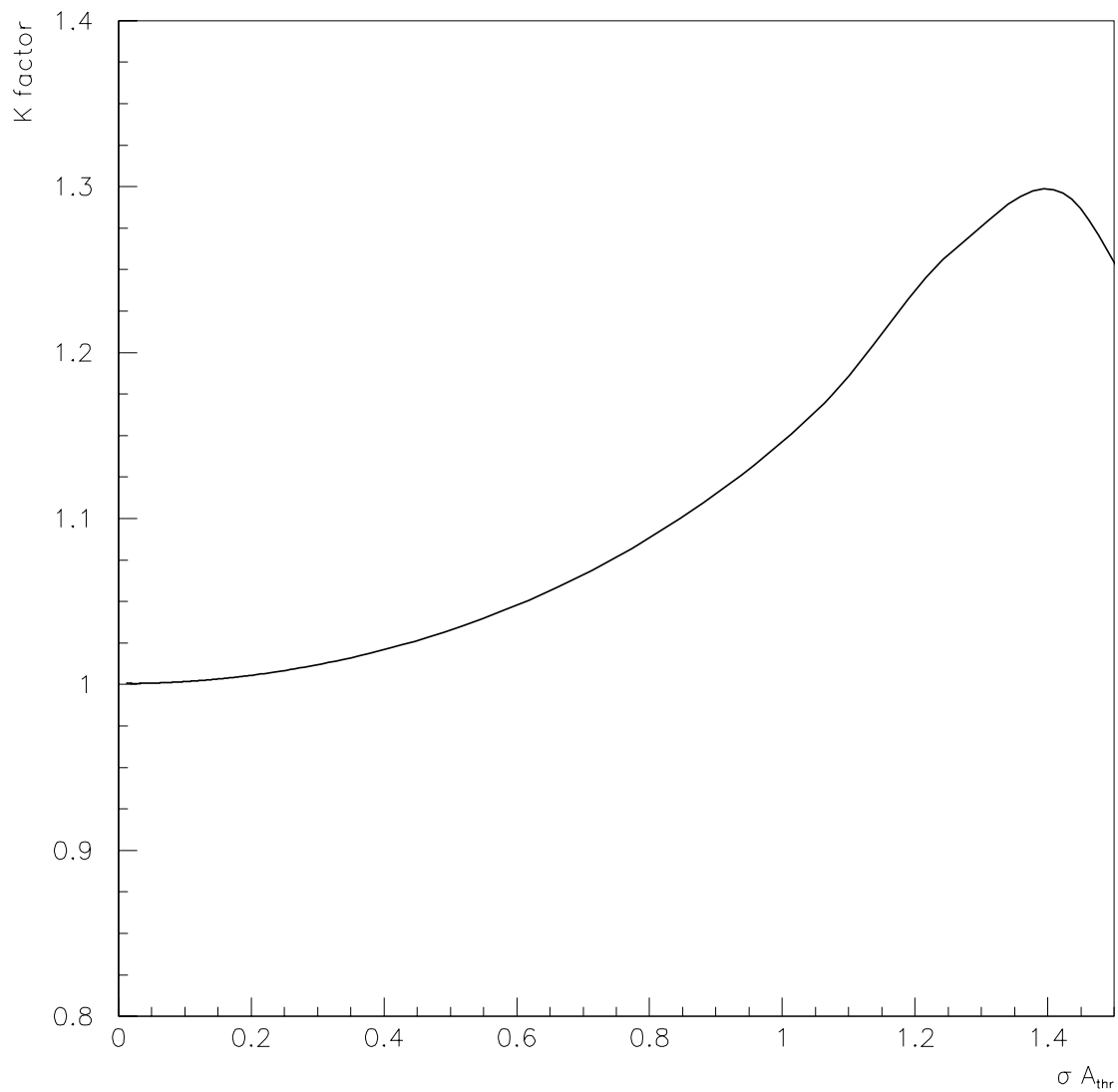


Fig. 2.— K factor versus magnification threshold  $A_{thr}$  times  $\sigma$ .  $\sigma$ , defined in section 4.1, is the ratio of the source size over the projection of the Einstein radius of the lens unto the source plane.